

ASASSN-18fk: A new WZ Sge-type dwarf nova with multiple rebrightenings and a new candidate for a superhumping intermediate polar

E. Pavlenko¹, K. Nijjima², P. Mason^{3,4}, N. Wells^{3,4}, A. Sosnovskij¹,
K. Antonyuk¹, A. Simon⁵, N. Pit¹, C. Littlefield⁶, H. Itoh⁷,
S. Kiyota⁸, T. Tordai⁹, P. Dubovsky¹⁰, T. Vanmunster¹¹, G. Stone¹²,
T. Kato², A. Sergeev^{13,14}, V. Godunova¹³, E. Lyumanov¹,
O. Antonyuk¹, A. Baklanov¹, Ju. Babina¹, K. Isogai²,
Ya. Romanyuk¹⁵, V. Troianskyi^{16,17} and V. Kashuba¹⁷

¹ Crimean astrophysical observatory of RAS, Republic of Crimea, (E-mail: eppavlenko@gmail.com)

² Department of Astronomy, Kyoto University, Kyoto 606-8502, Japan

³ New Mexico State University, MSC 3DA, Las Cruces, NM, 88003, USA

⁴ Picture Rocks Observatory, 1025 S. Solano, Suite D, Las Cruces, NM, 88001, USA

⁵ Astronomy and Space Physics Department, Taras Shevchenko National University of Kyiv, Volodymyrska str. 60, Kyiv, 01601, Ukraine

⁶ Department of Physics, University of Notre Dame, 225 Nieuwland Science Hall, Notre Dame, Indiana 46556, USA

⁷ Variable Star Observers League in Japan (VSOLJ), 1001-105 Nishiterakata, Hachioji, Tokyo 192-0153, Japan

⁸ VSOLJ, 7-1 Kitahatsutomi, Kamagaya, Chiba 273-0126, Japan

⁹ Polaris Observatory, Hungarian Astronomical Association, Laborc utca 2/c, 1037 Budapest, Hungary

¹⁰ Vihorlat Observatory, Mierova 4, 06601 Humenne, Slovakia

¹¹ Center for Backyard Astrophysics Belgium, Walhostraat 1A, B-3401 Landen, Belgium

¹² American Association of Variable Star Observers, 49 Bay State Rd., Cambridge, MA 02138, USA

¹³ ICAMER Observatory of NASU, 27 Acad. Zabolotnogo str., Kyiv, 03143, Ukraine

¹⁴ Terskol Branch of the Institute of Astronomy, Russian Academy of Science, Terskol, Kabardino-Balkarian Republic, 361605, Russian Federation

¹⁵ Main Astronomical Observatory of the National Academy of Sciences of Ukraine, 27 Acad. Zabolotnoho str., Kyiv, 03143, Ukraine

¹⁶ Institute Astronomical Observatory, Faculty of Physics, Adam Mickiewicz University in Poznan, ul. Sloneczna 36, PL60-286 Poznan, Poland

Received: November 20, 2018; Accepted: February 1, 2019

Abstract. We present the result of a multi-longitude campaign on the photometric study of the dwarf nova ASASSN-18fk during its superoutburst in 2018. It was observed with 18 telescopes at 15 sites during ~ 70 nights within a three-month interval. Observations covered the main outburst, six rebrightenings and 50-d decline to a near-quiet state. We identify ASASSN-18fk as WZ Sge-type dwarf nova with multiple rebrightenings and show the evolution of the 0.06-d superhump period over all stages of the superoutburst. A strong 22-min brightness modulation that superimposed on superhumps is found during rebrightenings and decline. Some evidence of this modulation in a form of a sideband signal is detected during the very onset of the outburst. We interpret the 22-min modulation as a spin period of the white dwarf and suggest that ASASSN-18fk is a good candidate for a superhumping intermediate polar.

Key words: accretion, accretion disks – cataclysmic variables – stars: dwarf novae – stars: individual: ASASSN-18fk

1. Introduction

Cataclysmic variables (CVs) are close binary systems which consist of an old (K-L) spectral type dwarf and a white dwarf (WD). The orbital periods of most of CVs are distributed between ~ 6 hours and ~ 76 -min period minimum (Hellier, 2001), (Knigge, 2006). There is the 2.15 -3.18 hr "period gap" with a deficiency of CVs within it.

The primary component, that is the WD, is accreting matter from the secondary old-type component, which filled its Roche Lobe and loses material via the inner Lagrangian point see e.g. (Warner, 1995) for CVs in general. Depending on the primary's magnetic field, accretion could occur through an accretion disk (non-magnetic CVs) or accretion stream is channelled onto magnetic poles (magnetic CVs or polars with magnetic field $B = 10^7 - 10^8$ G). Non-magnetic CVs (dwarf novae) display outbursts. SU UMa-type dwarf novae, which occupy a region of orbital periods 76 min – ~ 3 hr, possess the two types of outbursts – the normal ones and superoutbursts that are a result of the combination of thermal and tidal instabilities (Osaki, 1989); (Osaki, 1996). Typically, several normal outbursts that are shorter and slightly fainter than superoutbursts occur between two consecutive superoutbursts. The interval between superoutbursts varies between tens of days (SU UMa stars) and years – decades (WZ Sge type stars). More on the WZ Sge-type stars, see (Kato, 2015) for the review of these stars.

During superoutbursts, there are brightness variations (superhumps) with a period of several percent longer than the orbital one. Kato et al. (2009) in-

roduced three stages in the superhump evolution: stage A of the growing superhumps whose period is constant and slightly longer than the period at the next stage B; stage B with a systematically varying period and stage C with a shorter and almost constant period. One of the defining characteristics of WZ Sge-type dwarf novae are "early superhumps", the double-wave modulations during the early stage of the outburst with a period equal to the orbital one (Kato, 2002). Some WZ Sge-type stars may show so-called "late superhumps" – coherent modulation during the slowly fading stage (Kato et al., 2008).

The spin and orbital periods of the WD in magnetic CVs are synchronized (with an exception of four well-established, slightly asynchronous polars (Pavlenko et al., 2018). In the intermediate polars (IPs) the magnetic field of the white dwarf is $B = 10^6 - 10^7$ G and accretion occurs from an accretion ring onto the magnetic poles of the highly asynchronous white dwarf. Among 1166 CVs known up to 2012 (Ritter & Kolb, 2003), there are 38 of the confirmed IPs with some uncertainty of WZ Sge, see <http://asd.gsfc.nasa.gov/Koji.Mukai/iphone/iphone.htm>; Woudt et al. (2012). The orbital periods of the known IPs are distributed between 81 and 1000 min, where the most of them have the orbital period above the period gap. Only eight IPs are placed below the period gap, which include six outbursting members (Woudt et al., 2012). The only outbursting IPs with superhumps are V455 And, CC Scl and possibly WZ Sge.

ASASSN-18fk was discovered on March 17 by the ASASSN-team as a bright star of $12^m.14$. It matched the blue $g = 19^m.6$ SDSS source (VSNET-alert 21987) and according to the CRTS data showed no past outbursts. C. Littlefield reported on the 0.0570(3) d modulation (VSNET-alert 21992) that was preliminary identified as double-wave early superhumps of a likely new WZ Sge-type dwarf nova, ASASSN-18fk. Here, we report results of the multisite campaign of the ASASSN-18fk investigation during the superoutburst and its decline up to the near-quiescent state.

2. Observations

The CCD-photometry of ASASSN-18fk was done in 2018 with 18 telescopes located at 15 observatories during 70 nights (see Table 1). All observations were obtained in unfiltered light. CCD frames were dark subtracted and flat-fielded in the usual manner. Depending on a size of the telescope, time exposure, weather conditions and brightness of the object, the accuracy of a single observation varied between $0^m.005$ and $0^m.007$. All the data were measured relative to the comparison star 148 ($\alpha_{2000} = 12^h08^m53.45^s$, $\delta_{2000} = 19^\circ16'05.6''$) in the AAVSO designation, $V = 14^m.813$, $B - V = 0^m.792$ from the sequence X23128MX (AAVSO) and expressed in the Heliocentric Julian Day (HJD). During the time of our observations, the brightness of ASASSN-18fk decreased from $13^m.3$ to $19^m.5$.

Table 1.: Journal of observations.

HJD 2458000+ (start - end)	Observatory/telescope	CCD	N
195.587 - 195.821	LCO/0.80m	SBIG STL-1001E	1543
199.409 - 199.599	DPV/1m	MII G2-1600	244
199.566 - 199.799	LCO/0.80m	SBIG STL-1001E	1078
200.287 - 200.440	DPV/1m	MII G2-1600	196
200.303 - 200.408	Trt/0.25m	ALCCD 5.2 (QHY6)	263
200.570 - 200.682	LCO/0.80m	SBIG STL-1001E	520
201.423 - 201.627	DPV/1m	MII G2-1600	263
201.501 - 201.572	Trt/0.25m	ALCCD 5.2 (QHY6)	135
202.048 - 202.322	Ioh/0.25m	SBIG ST-9XE	440
202.077 - 202.211	Kis/0.25m	APOGEE F47	263
202.293 - 202.408	Trt/0.25m	ALCCD 5.2 (QHY6)	544
202.388 - 202.511	Van/0.40m	SBIG ST-10XME	89
202.401 - 202.610	DPV/1m	MII G2-1600	254
202.935 - 202.999	Kis/0.25m	APOGEE F47	117
203.000 - 203.209	Kis/0.25m	APOGEE F47	480
203.003 - 203.290	Ioh/0.25m	SBIG ST-9XE	455
203.227 - 203.534	CrAO/0.38m	APOGEE E47	436
203.976 - 203.999	Ioh/0.25m	SBIG ST-9XE	39
204.000 - 204.030	Ioh/0.25m	SBIG ST-9XE	49
204.037 - 204.240	Kis/0.25m	APOGEE E47	468
204.937 - 204.999	Ioh/0.25m	SBIG ST-9XE	80
205.000 - 205.031	Ioh/0.25m	SBIG ST-9XE	51
206.024 - 206.233	Kis/0.25m	APOGEE E47	484
212.227 - 212.453	CrAO/0.38m	APOGEE E47	160
213.224 - 213.547	CrAO/0.38m	APOGEE E47	216
215.311 - 215.584	CrAO/0.38m	APOGEE E47	193
216.238 - 216.503	CrAO/0.38m	APOGEE E47	188
217.284 - 217.445	CrAO/0.38m	APOGEE E47	114
219.229 - 219.338	CrAO/2.6m	APOGEE E47	733
220.247 - 220.379	CrAO/2.6m	APOGEE E47	724
221.288 - 221.425	CrAO/1.25m	ProLine PL23042	847
222.279 - 222.377	CrAO/1.25m	ProLine PL23042	250
223.263 - 223.390	CrAO/1.25m	ProLine PL23042	86
224.270 - 224.387	CrAO/1.25m	ProLine PL23042	293
226.297 - 226.446	CrAO/1.25m	ProLine PL23042	71
228.303 - 228.310	CrAO/1.25m	ProLine PL23042	19
229.262 - 229.380	CrAO/1.25m	ProLine PL23042	272
230.264 - 230.392	CrAO/1.25m	ProLine PL23042	89
230.395 - 230.539	Terskol/0.6m	SBIG STL-1001	296
231.249 - 231.478	Terskol/0.6m	SBIG STL-1001	195
231.257 - 231.390	CrAO/1.25m	ProLine PL23042	179
232.362 - 232.484	CrAO/1.25m	ProLine PL23042	165
233.296 - 233.420	Terskol/0.6m	SBIG STL-1001	269
233.309 - 233.461	CrAO/1.25m	ProLine PL23042	72
234.290 - 234.373	CrAO/1.25m	ProLine PL23042	35
235.363 - 235.465	CrAO/1.25m	ProLine PL23042	138
236.356 - 236.378	CrAO/1.25m	ProLine PL23042	31
237.338 - 237.353	CrAO/1.25m	ProLine PL23042	41
238.288 - 238.308	CrAO/1.25m	ProLine PL23042	45
239.270 - 239.397	CrAO/1.25m	ProLine PL23042	90
239.291 - 239.401	Lisnyky/0.35m	SBIG ST-8XMEI	88
240.338 - 240.340	Lisnyky/0.7m	ProLine PL4710	6

Table 1.: Journal of observations (continued).

HJD 2458000+ (start - end)	Observatory/telescope	CCD	N
240.346 - 240.352	Terskol/0.6m	SBIG STL-1001	222
241.311 - 241.314	Lisnyky/0.7m	ProLine PL4710	5
242.282 - 242.412	CrAO/0.38m	APOGEE E47	63
242.324 - 242.382	Lisnyky/0.7m	ProLine PL4710	166
243.290 - 243.428	CrAO/0.38m	APOGEE E47	66
243.307 - 243.311	Lisnyky/0.7m	ProLine PL4710	5
244.414 - 244.506	Mayaky/0.8m	MicroLine 9000	104
245.251 - 245.525	CrAO/0.38m	APOGEE E47	127
249.315 - 249.507	Lisnyky/0.35m	SBIG ST-8XMEI	179
251.285 - 251.343	CrAO/1.25m	ProLine PL23042	24
252.289 - 252.359	CrAO/1.25m	ProLine PL23042	34
253.413 - 253.487	Mayaky/0.8m	MicroLine 9000	72
254.295 - 254.400	CrAO/1.25m	ProLine PL23042	49
259.331 - 259.380	CrAO/1.25m	ProLine PL23042	24
260.278 - 260.452	CrAO/2.6m	APOGEE E47	259
261.278 - 261.310	CrAO/2.6m	APOGEE E47	43
278.288 - 278.377	CrAO/2.6m	APOGEE E47	121
279.282 - 279.359	CrAO/2.6m	APOGEE E47	107
287.641 - 287.731	McDonald/2.1m	ProEM	1560

Description of columns:

HJD 2458000+ (start-end): beginning and end of an observational run.

Observatory/telescope: LCO - C.Littlefield, DPV - P.Dubovsky, Trt - T.Tordai, Ioh - H.Itoh, Kis - S.Kiyota, Van - T.Vanmunster; CrAO - Crimean Astrophys. Obs., Lisnyky - Lisnyky Obs., Terskol - Terskol Obs., Mayaky - Mayaki Obs., McDonald - Picture Rocks Obs.

CCD: CCD camera type. N: number of observations.

3. Superoutburst and superhumps

The overall light curve of ASASSN-18fk during the superoutburst is presented in Fig. 1. It includes the main outburst, six rebrightenings and the ~ 50 -d decline to the near-quietest state. Taking into account the ASASSN data, one could conclude that the superoutburst amplitude was about 7^m and the main outburst lasted for ~ 15 d. The amplitude of rebrightenings was $\sim 3^m$. It seems that ~ 100 d after the start of the outburst, ASASSN-18fk reached its quiescence, or at least appeared close to it.

In the course of the main outburst, rebrightenings and superoutburst decline, the superhumps have been observed. The early superhumps, having a two-humped profile, were detected only for JD 2458195 with a period of 0.057-0.060 d. A further gap in the observations did not allow us to estimate the duration of this stage. Using both the periodogram analysis (Pelt, 1992) and O-C method for the superhump maxima, we identified a stage of growing superhumps A, with a period of 0.06075(2) d and a stage of fully developed superhumps B, with a near-constant mean period of 0.05940(1) d. The stage A lasted for at least about 20 cycles, while stage B – about 60 cycles (see Fig. 2).

The lack of data at the stage of early superhumps did not ensure sufficient accuracy in estimating the period that could be considered as the orbital one, and, hence, in

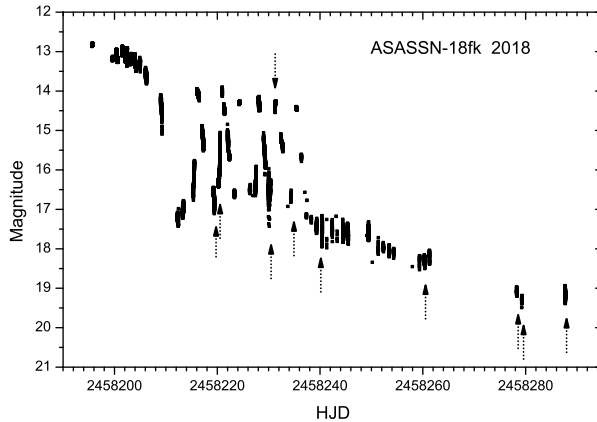


Figure 1. The overall light curve. The dates when the 0.015-d period was detected are shown by arrows.

defining the binary mass ratio, using the method proposed by Kato & Osaki (2013). During the stages of rebrightenings and superoutburst decline, the period of superhumps was 0.059586(7) d and 0.059521(4) d, respectively, that is 0.3% - 0.2% larger than the period during stage B. We suggest that this period probably could be a period of late superhumps similar to what was observed in three WZ Sge-like stars GW Lib, V455 And and WZ Sge (Kato et al., 2008). No orbital periodicity was detected after the main outburst termination.

Taking into account the outburst features described, ASASSN-18fk could be defined as a WZ Sge-type dwarf nova with multiple rebrightenings – type B outburst according to the classification given by Kato (2015).

4. Short-periodic variations

We found that additionally to the 0.06-d superhumps the nights of the best quality displayed a short-term 22-min brightness variability at different stages of the superoutburst – during rebrightenings and superoutburst decline. This modulation was not seen during the main outburst.

We considered a short-term periodicity for these stages separately. We constructed the periodograms for these selected data using the ISDA package (Pelt, 1992) after removing a superhump wave and a trend corresponding to the superoutburst profile. The original light curves for these nights and periodograms for the detrended data are shown in Fig. 3, and in Fig. 4, for the outburst decline stage. All the periodograms contain the strongest peak around 0.015 d (22 min) with an exception of the first night where the 0.015-d period has the second rating. Contrary to the 0.015-d period that was detected at the rebrightening stage, these data contain a signal at the first harmonic of the 0.015-d period which became stronger as ASASSN-18fk approached the quiescence.

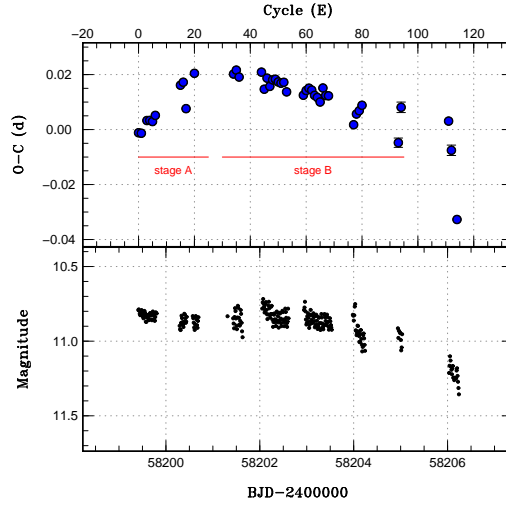


Figure 2. Evolution of superhumps. Upper panel: O-C for the superhump maxima. Stages A and B are marked. Lower panel: a part of the main outburst.

We assume that these short-periodic variations may be related to the spin period of the WD. Therefore, ASASSN-18fk could be classified as an intermediate polar (IP). Another evidence in favor of the IP is a modulation around $\sim 50d^{-1}$ (for JD=2458195 and JD=2458199) and at $\sim 84d^{-1}$ (for JD=2458219 and JD=2458260) that coincides with beat frequencies $\omega - \Omega$ and $\omega + \Omega$ between 0.06-d and 0.015-d periods (see Fig.5, Fig.3 and Fig.4), where ω and Ω are spin and orbital frequencies, respectively. The possibility of existence of the spin-orbital sidebands of $\omega \pm \Omega$ for IPs was predicted earlier by Warner (1986) and Wynn & King (1992). Note that although a precise orbital frequency is unknown, we could roughly admit it to be close to the 0.06-d superhump period.

5. The place of ASASSN-18fk among outbursting IPs

Due to our preliminary classification, several questions arise concerning the period coherence, its profile, change of amplitude in the range from rebrightenings to the late decline and place in a space of orbital – spin periods among outbursting IPs.

5.1. Is the 0.015-d periodicity coherent throughout the main outburst, rebrightenings and outburst decline?

Fig. 6 shows the examples of the phase light curves folded on the 0.015-d period for the data between rebrightenings, at the top of the rebrightening and close to the quiescent state.

It is seen that the 0.015-d modulation was highly coherent during the outburst decline, but it was not coherent during the stage of rebrightenings. The magnetosphere

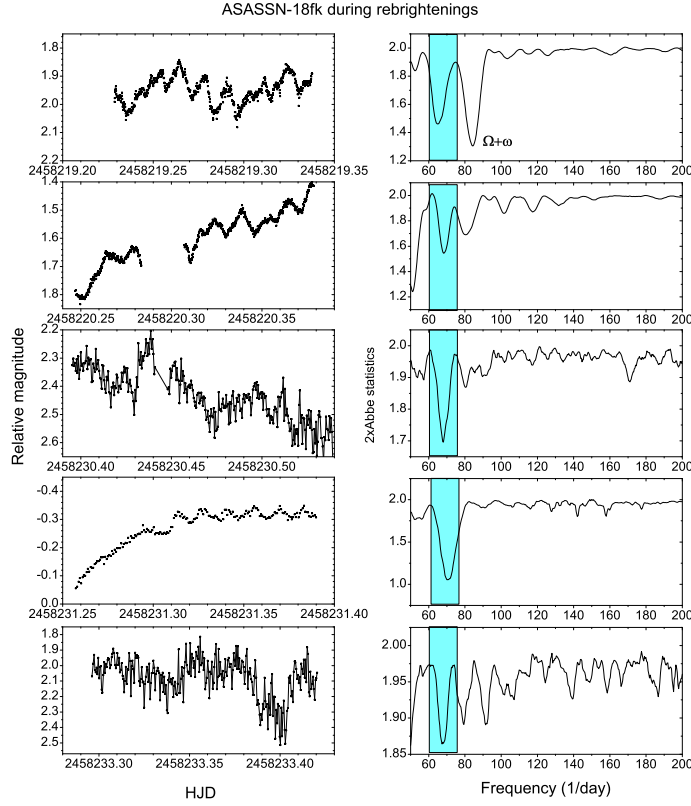


Figure 3. Left: examples of original nightly light curves for the rebrightening stage displaying the 0.015-d period. Right: corresponding periodograms. The region around the 0.015-d period is marked by the blue strip.

radius of the white dwarf varied on a scale of days during rebrightenings and, as a whole, it was smaller than during the late stage of the outburst decline, when the magnetosphere was rather "quiet". Obviously, it will produce both different accretion geometry and visibility of accretion regions between these two stages. It is known that another IP, DO Dra, displayed an unstable profile of the spin period and a significant shift of the peak at the spin frequency in periodograms for some nights (Szkody et al., 2002); (Andronov et al., 2008).

5.2. Is a difference between spin profiles at high and low brightness stages common for the IPs?

As shown in Section 4, ASASSN-18fk displayed a one-humped spin profile during rebrightenings and a two-humped one during the outburst decline. Most of the known outbursting IPs exhibit the same behavior. One explanation of this phenomenon was

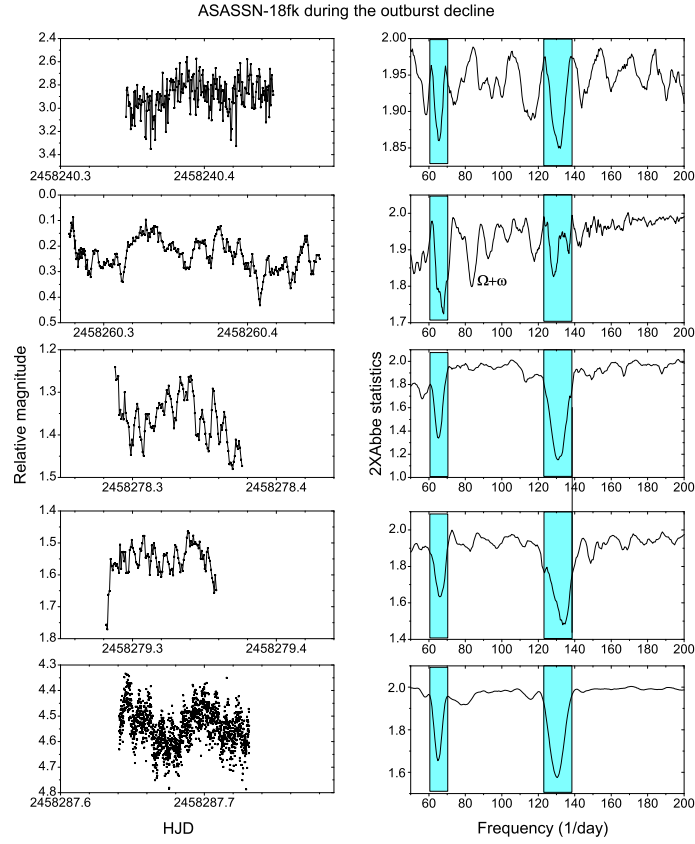


Figure 4. Left: examples of original nightly light curves for the superoutburst decline stage displaying the 0.015-d period. Right: corresponding periodograms. The regions around the 0.015-d period and its first harmonic are marked by the blue strip.

given for XY Ari by Hellier et al. (1997): humps on the spin light curve are associated with two accretion regions on a white dwarf. In quiescence, the magnetosphere radius is rather large and two zones are visible. In outburst, the magnetosphere is reduced by a higher accretion rate and the accretion disk obscures one of the poles. However, as noted by Hellier (2001), "Currently, we do not have enough observational clues to determine why some systems show double-peaked pulses while others are single peaked".

5.3. What is an amplitude of the spin pulse at different stages of the superoutburst?

The mean amplitude of the 0.015-d period was about $0^m.04$ at the stage of rebrightenings and $0^m.09$ during the gradual decline stage. Converting magnitudes into rel-

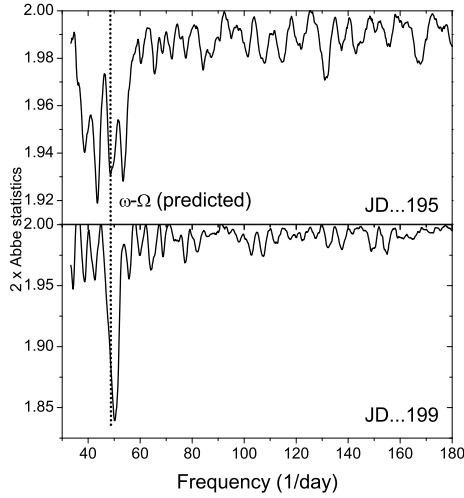


Figure 5. Periodograms for the data during two nights of observations: JD 2458195 (above) and JD 2458199 (below). The dotted line indicates a position of the side-band $\omega - \Omega$ frequency. The last three numbers of JD are given for the date of observations.

ative intensities, we found a dependence of the amplitude of the mean spin pulse of ASASSN-18fk on the mean brightness (see Fig. 7). At the top of the rebrightening, the spin amplitude was three times larger than those between rebrightenings and ~ 50 times larger than those at the end of the outburst decline. The tendency of a growing amplitude with brightness is not common for all outbursting IPs. Thus, there is no significant difference in the spin amplitudes for outbursts and quiescence for DO Dra, but there is a similar dependence for XY Ari (Hellier et al., 1997).

5.4. What is a position of ASASSN-18fk in the $P_{orb} - P_{spin}$ diagram?

We used the available data (Woudt et al., 2012) and our estimate for ASASSN-18fk to plot a dependence of the spin period on the orbital one for all IPs below the period gap. Taking into account that the expected orbital period for ASASSN-18fk is slightly lower than the superhump period, we could use the mean superhump period value as an estimate of the orbital one. In this case the spin period is ~ 3.8 times smaller than the orbital one, that is close to the values of the known IPs below the period gap (Woudt et al., 2012). The position of ASASSN-18fk among these IPs is shown in Fig. 8. While IPs above the period gap are on or below the line of $P_{spin} = 0.1P_{orb}$ (Hellier, 2001), IPs with the shortest orbital period (excepting EX Hya) are concentrated within a strip on either side of this line. ASASSN-18fk is situated well within this strip.

6. Conclusion

Our main findings for ASASSN-18fk are as follows:

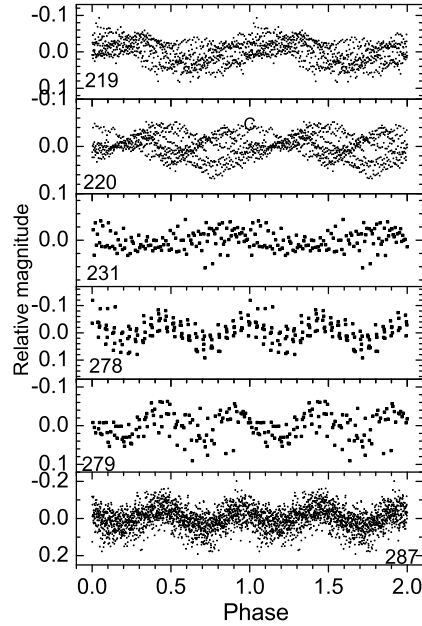


Figure 6. The detrended data folded on the 0.0153492-d period with zero-epoch HJD=2458219.22859. The last three numbers of JD are given for the date of observations. The light curves from the top to bottom correspond to the observations between the first and second rebrightening (JD ...219), during the rise to the second rebrightening (JD ...220), during the top of the fifth rebrightening (JD ...231) and during the superoutburst decline (JD ...278, ...279 and ...287).

1) ASASSN-18fk is a WZ Sge-type dwarf nova with six rebrightenings and a superhump period of 0.06-d; 2) the one-humped 22-min signal was detected during the rebrightening stage and the two-humped one – during the outburst decline, which is assumed to be the spin period of the white dwarf; 3) spin-orbital sideband periods during the main outburst.

Thus ASASSN-18fk is a first IP among the rare subclass of the superhumping IPs for which evidence of the spin period (the direct spin signal or the spin-orbital sideband signal) was tracked through the main outburst, rebrightenings and near-quietest state.

References

- Andronov, I. L., Chinarova, L. L., Han, W., Kim, Y., & Yoon, J. N., Multiple timescales in cataclysmic binaries. The low-field magnetic dwarf nova DO Draconis. 2008, *Astron. Astrophys.*, **486**, 855, DOI: 10.1051/0004-6361:20079056
- Hellier, C. 2001, *Cataclysmic Variable Stars*

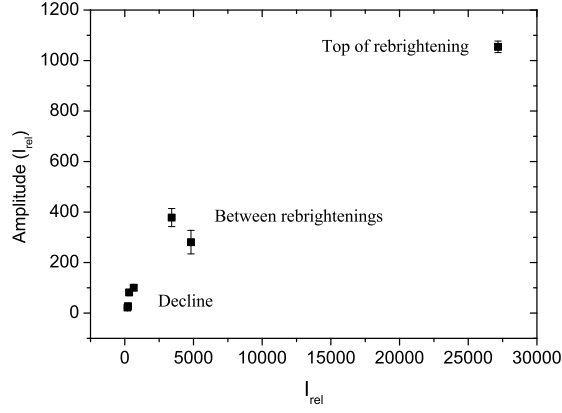


Figure 7. Dependence of the amplitude of the 0.015-d modulation expressed in the relative intensity (I_{rel}) on the mean relative intensity from the decline to the top of rebrightening ($I_{rel} = 10^{10} \times 10^{-0.4m}$).

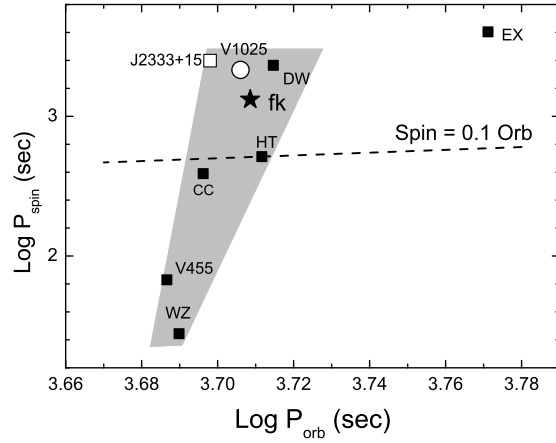


Figure 8. Dependence between spin and orbital periods for the IPs below the period gap. Abbreviations mean: EX = EX Hya; J2333+15 = SDSS J2333+15; V1025 = V1025 Cen; DW = DW Cnc; HT = HT Cam, V455 = V455 And; CC = CC Scl; fk = ASASSN-18fk. SDSS J2333+15 with no information on possible outburst and V1025 Cen are marked by the open square and circle, respectively. The rest are outbursting IPs. ASASSN-18fk is marked by a star symbol. The dashed line corresponds to the $P_{spin} = 0.1P_{orb}$ relation. Gray area indicates location of IPs below the period gap (with an exception of EX Hya).

- Hellier, C., Mukai, K., & Beardmore, A. P., An outburst of the magnetic cataclysmic variable XY ARIETIS observed with RXTE. 1997, *Mon. Not. R. Astron. Soc.*, **292**, 397, DOI: 10.1093/mnras/292.2.397
- Kato, T., On the Origin of Early Superhumps in WZ Sge-Type Stars. 2002, *Publications of the Astronomical Society of Japan*, **54**, L11, DOI: 10.1093/pasj/54.2.L11
- Kato, T., WZ Sge-type dwarf novae. 2015, *Publications of the Astronomical Society of Japan*, **67**, 108, DOI: 10.1093/pasj/psv077
- Kato, T., Imada, A., Uemura, M., et al., Survey of Period Variations of Superhumps in SU UMa-Type Dwarf Novae. 2009, *Publications of the Astronomical Society of Japan*, **61**, S395, DOI: 10.1093/pasj/61.sp2.S395
- Kato, T., Maehara, H., & Monard, B., Late Superhumps in WZ Sge-Type Dwarf Novae. 2008, *Publications of the Astronomical Society of Japan*, **60**, L23, DOI: 10.1093/pasj/60.4.L23
- Kato, T. & Osaki, Y., New Method of Estimating Binary's Mass Ratios by Using Superhumps. 2013, *Publications of the Astronomical Society of Japan*, **65**, 115, DOI: 10.1093/pasj/65.6.115
- Knigge, C., The donor stars of cataclysmic variables. 2006, *Mon. Not. R. Astron. Soc.*, **373**, 484, DOI: 10.1111/j.1365-2966.2006.11096.x
- Osaki, Y., A model for the superoutburst phenomenon of SU Ursae MAJoris stars. 1989, *Publications of the Astronomical Society of Japan*, **41**, 1005
- Osaki, Y., Dwarf-Nova Outbursts. 1996, *Publications of the Astronomical Society of the Pacific*, **108**, 39, DOI: 10.1086/133689
- Pavlenko, E. P., Mason, P. A., Sosnovskij, A. A., et al., Asynchronous polar V1500 Cyg: orbital, spin, and beat periods. 2018, *Mon. Not. R. Astron. Soc.*, **479**, 341, DOI: 10.1093/mnras/sty1494
- Pelt, J. 1992, *Irregularly Spaced Data Analysis User Manual*
- Ritter, H. & Kolb, U., Catalogue of cataclysmic binaries, low-mass X-ray binaries and related objects (Seventh edition). 2003, *Astron. Astrophys.*, **404**, 301, DOI: 10.1051/0004-6361:20030330
- Szkody, P., Nishikida, K., Erb, D., et al., X-Ray/Optical Studies of Two Outbursts of the Intermediate Polar YY (DO) Draconis. 2002, *Astron. J.*, **123**, 413, DOI: 10.1086/324733
- Warner, B., Multiple optical orbital sidebands in intermediate polars. 1986, *Mon. Not. R. Astron. Soc.*, **219**, 347, DOI: 10.1093/mnras/219.2.347
- Warner, B., Cataclysmic variable stars. 1995, *Cambridge Astrophysics Series*, **28**
- Woudt, P. A., Warner, B., Gulbis, A., et al., CC Sculptoris: a superhumping intermediate polar. 2012, *Mon. Not. R. Astron. Soc.*, **427**, 1004, DOI: 10.1111/j.1365-2966.2012.22010.x
- Wynn, G. A. & King, A. R., Theoretical X-ray power spectra of intermediate polars. 1992, *Mon. Not. R. Astron. Soc.*, **255**, 83, DOI: 10.1093/mnras/255.1.83